2019 SECED Conference
Earthquake risk and engineering towards a resilient world
9-10 September 2019, Greenwich, London

SCENARIO-BASED PROBABILISTIC SEISMIC PERFORMANCE ANALYSIS OF AN ARCHETYPAL TALL BUILDING IN ISTANBUL USING PHYSICS-BASED EARTHQUAKE GROUND MOTION SIMULATIONS

Ömer Odabaşı[1], Paolo F. Bazzurro[2], Maria Infantino[3], Chiara Smerzini[4] & Marco Stupazzini[5]

Abstract: *Due to the increasing availability of high-performance computational resources, physics-based ground motion simulations (PBGMS) are becoming viable alternatives to ground-motion recordings as input to structural response analysis. One of the primary advantages of the simulated ground motions is that they are site-specific because they reflect the seismic source process, the propagation path and local site characteristics of potential causative earthquake scenarios that might occur in the region of interest. In this paper, we assessed the seismic performance of a 23-storey tall building archetype designed as per post-1980 modern capacity design principles at three different sites in Istanbul under a magnitude M_w=7.2 earthquake scenario. Considering the seismic gap in the Sea of Marmara, it is advocated amongst informed researchers that this scenario could manifest itself as the 'next big one'. We evaluated the seismic performance of the archetype via (1) conventional methods using recorded ground motions that match empirically predicted target acceleration response spectra, and (2) physics-based simulations (PBS) using the spectra element code SPEED (http://speed.mox.polimi.it). We observed that the PBS are, on average, more aggressive than the suites of recorded motions. Further, the PBS resulted in much smaller dispersions in the distributions of structural demands. Consequently, depending on the building site, economic losses that the archetype might suffer due to the scenario event averaged between 3-to-18% of the total replacement cost via the conventional approach, and 10-to-23% via PBS.*

Introduction

Earthquake engineers are often interested in assessing the seismic performance of engineering structures under strong earthquake ground shakings. Historically, recorded accelerograms from past events have been extensively used as input time series in dynamic analyses to achieve this objective. However, damaging earthquakes rarely occur, therefore there is a limited number of recordings representative of specific scenario ruptures of interest. To work around this problem, the expected shaking is characterized in terms of relevant intensity measures using empirically calibrated ground motion predictive models (GMPM), and ground-motion records, which are garnered in global or regional databases (e.g., NGA West-2 database: https://ngawest2.berkeley.edu/), are selected and scaled to match the computed target distribution. This approach has well matured over many decades, and now they are conventionally practiced by analysts. However, the limitations associated with factors such as the ergodic assumption in the GMPEs due to the scarcity of observational evidence and amplitude scaling of recorded accelerograms cannot be overlooked.

Numerical simulation of the ground motion is becoming prevalent with the current progresses made regarding the underlying models and computational resource capabilities. Physics-based simulations (PBS), in particular, represent a great promise for addressing many of the limitations of the conventional methods that rely on ergodic empirical models for ground motion prediction

[1] PhD student, University School of Advanced Studies of Pavia (IUSS), Pavia, Italy, omer.odabasi@iusspavia.it
[2] Professor, University School of Advanced Studies of Pavia (IUSS), Pavia, Italy, paolo.bazzurro@iusspavia.it
[3] PhD student, Politecnico di Milano, Milano, Italy, maria.infantino@polimi.it
[4] Researcher, PhD, Politecnico di Milano, Milano, Italy, chiara.smerzini@polimi.it
[5] Consultant, Munich RE, Munich, Germany, MStupazzini@munichre.com

and scaled accelerograms for dynamic analyses. The *CyberShake* platform (Graves et al., 2011) by the Southern California Earthquake Center (SCEC), the QuakeCore program and its subsidiary *Cybershake NZ* project (Tarbali et al., 2018) in New Zealand and the *SPEED* engine (Mazzieri et al., 2013) by Politecnico di Milano constitute some of the eminent contributors to the developments in this field. Furthermore, there has also been notable activity pertaining to the validation of PBS (e.g., Baker *et al.*, 2014; Bradley *et al.*, 2017).

Predicting near-fault ground motions that are caused by large crustal earthquakes via the existing empirical models can be particularly unreliable depending on the geospatial relation between the rupture plane and the recording site. In this regard, directivity effects (Shahi and Baker, 2011; Somerville et al., 1997) and strong polarization (i.e., directionality of ground motion: Bradley and Baker, 2014) of the motion are amongst the major impediments. In addition, appropriate consideration of these phenomena during record selection is still an equally challenging task. On the other hand, physics-based ground motion simulations carry the signature of the source, path and local soil characteristics of the associated earthquake rupture (Paolucci et al., 2015). For example, the variation in the shaking at a site related to the uncertainties in the source parameters such as hypocentre location, slip distribution and stress drop are delineated through multiple realizations of the same rupture.

In this paper, we assessed the seismic performance of a tall building archetype at three different sites in Istanbul via PBS and compared the results to those obtained via the conventional approach outlined in the previous paragraphs. The scenario rupture that we used for the assessments stretches across the Central Marmara segments of the North Anatolian Fault (NAF) system, and it has a moment magnitude, M_w=7.2. The selected sites constitute different levels of expected shaking intensity, local site conditions and spatial relations with respect to the rupture plane. Fifteen 3D ground motion simulations are generated using the SPEED engine (http://speed.mox.polimi.it) for fifteen realizations of the same rupture plane delineating the variations in the earthquake source, path and local site conditions. On the other hand, through the conventional approach, which represents the benchmark case, fifteen ground motion pairs are selected and scaled to match the empirically predicted target spectrum using the GMPM of Boore et al. (2014). Using only the horizontal components of the ground motions as input time series, dynamic analyses are performed to evaluate and compare relevant engineering demand parameter distributions, simple global damage and loss predictions.

The seismic landscape surrounding Istanbul

Istanbul is located in a seismically active area because of its proximity to the North Anatolian Fault (NAF) and its subsidiary branching segments across Marmara Region. The long-term seismicity is illustrated in Figure 1. Earthquake recordings spanning the last two millennia in the region indicated that, on average, every 50 years a medium intensity (MMI: VII-VIII, Wood and Neumann, 1931) earthquake occurred (Ambraseys and Finkel, 1991). Furthermore, the return period of severe earthquakes characterized by high levels of macro-intensity (MMI: VIII-IX) was around 300 years (Erdik et al., 2004). In 1999, two devastating earthquakes struck the region. The Marmara earthquake (Mw=7.4) occurred in 17 August in the city of İzmit, roughly 100 km to east from Istanbul. The ground-motion was felt in the city to varying degrees. Structural damage were reported on the European side of Istanbul at sites with relatively loose soil conditions. The Düzce earthquake on November had a M_w magnitude 7.2. Its epicentre was approximately 200 km away from Istanbul. Dönmez and Pujol (2005) reported that in Düzce, approximately 40% of the entire building stock either suffered extensive damage or collapsed after the two earthquakes.

Projecting towards near future, there is a concerning prediction amongst informed academics that the seismic gap in the Sea of Marmara heightens the odds of a large earthquake occurring along the Central Marmara segments of the North Anatolian Fault Zone (NAFZ) (Bohnhoff et al., 2016; Parsons et al., 2000). This claim was supported by the fact that the series of past earthquakes along the NAFZ since 1776 had occurred in a domino-like fashion propagating from east to west. In fact, Parsons et al. computed that probability that the probability of a M>7.0 earthquake occurring in greater Istanbul between the years 2000-to-2030 would be 62±15%.

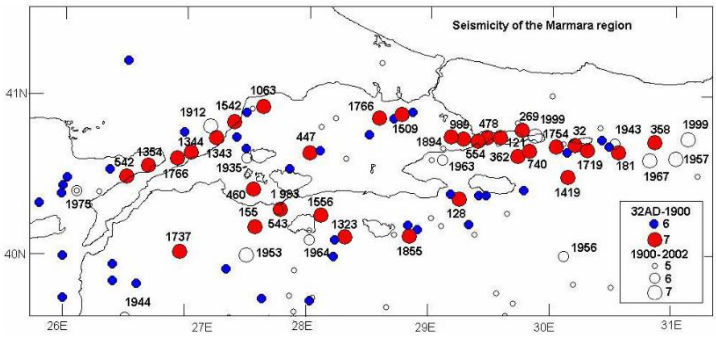

Figure 1. Seismicity of the Marmara Region. Taken from Ambraseys and Finkel (1991)

Case study description

The probabilistic scenario-based seismic demand and response assessment undertaken herein comprises two different approaches: physics-based and conventional. The former uses numerically simulated ground motions as input time series in dynamic analyses, whereas the latter selects and scales real recordings to perform the same task. Figure 2 illustrates the case study area, considered fault rupture plane and the three sites for which the computations are performed. Detailed description of the scenario earthquake rupture and building sites for seismic demand and performance analyses are presented in the following paragraphs.

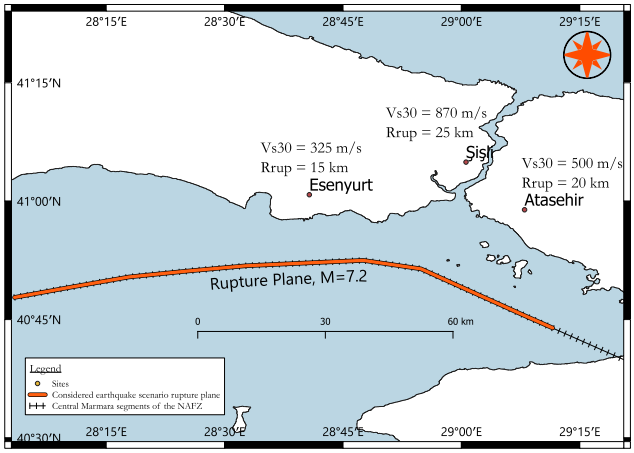

Figure 2. Illustration of the case study area, projection of earthquake rupture plane and building sites

Considered Earthquake Rupture Scenario

In view of the seismotectonic setting surrounding Istanbul, we decided to base our scenario evaluation to a magnitude M_w=7.2 strike-slip earthquake rupturing along three subsidiary branches (Central Marmara segments) of the NAFZ located to the south of the city. According to Bohnhoff et al. (2016) this scenario, or one of its variants, could potentially be the next 'big one'. The dimensions of the rupture plane are 84-by-15 kilometres (slip-dip), and it cuts through the ground. That is to say the upper seismogenic depth of the fault rupture is zero.

Building Sites

The impact of the scenario earthquake on the city of Istanbul can reach catastrophic levels in different parts of the city because of a few major reasons. First, the population and the building stock is concentrated in the southern shoreline, i.e. closer to the earthquake source, thus increasing the expected level of ground shaking across the whole spectrum of vibration periods of engineering interest. Second, significant amplification of the ground motion can be expected across the southern shoreline of the European side of the city where the soil is comparatively looser. Moreover, because of its unfortunate geospatial alignment, forward-directivity effects might be prevalent across both sides of the city (Paolucci et al., 2017). This phenomenon manifest itself in the form of large velocity pulses in the ground motions. The probability of observing a pulse-like shaking at a given site is known to be a function of both the position of the site and the

direction of the rupture propagation. Further, the period of the pulse is tightly related to the size of the rupture plane, and thus the magnitude (Shahi and Baker, 2011). To this end, we selected three sites, which are shown in Figure 2, that: (1) represent locations where tall buildings are densely populated, (2) have varying levels of seismic hazard, (3) constitute different levels of susceptibility to pulse-like ground motion, and (4) different local site conditions.

Conventional approach: scaled ground motions

Traditional scenario-based probabilistic seismic demand analysis relies on empirical ground-motion predictive models (GMPMs) for selecting and scaling ground motion records. Distributions of relevant shaking intensities (almost always only spectral accelerations) of the scaled records must follow those predicted by the GMPM using the causal parameters of the considered earthquake scenario. Herein, we used the model of Boore et al. (2014) to predict the 5% damped spectral accelerations for periods between 0.1 to 5 seconds. The model computes the spectra as median single-component horizontal ground motion across all non-redundant azimuths: Sa_{RotD50} (Boore et al., 2006). Then, using the NGA-West2 database, 15 ground motions pairs are selected and scaled to match the target distributions at the building sites. Note that the Sa_{RotD50} properties across the above-mentioned period range of the recordings are used in the process. Moreover, we filtered the database by causal earthquake parameters and soil conditions at the stations of the recordings to enforce, implicitly, consistency in the distributions of non-spectral intensity measures such as ground-motion duration. The allowed ranges of magnitude, distance and soil conditions are: M = 7.2 ± 0.25, R = $R_{rup,site}$ ± 15 km (and R>5 km), and V_{s30} = $V_{s30,site}$ ± 250 m/s. Figure 3 illustrates the spectra of the selected and scaled records, their distributions, and the target spectra predicted by the GMPM. These records form the basis of evaluations via the 'conventional approach'.

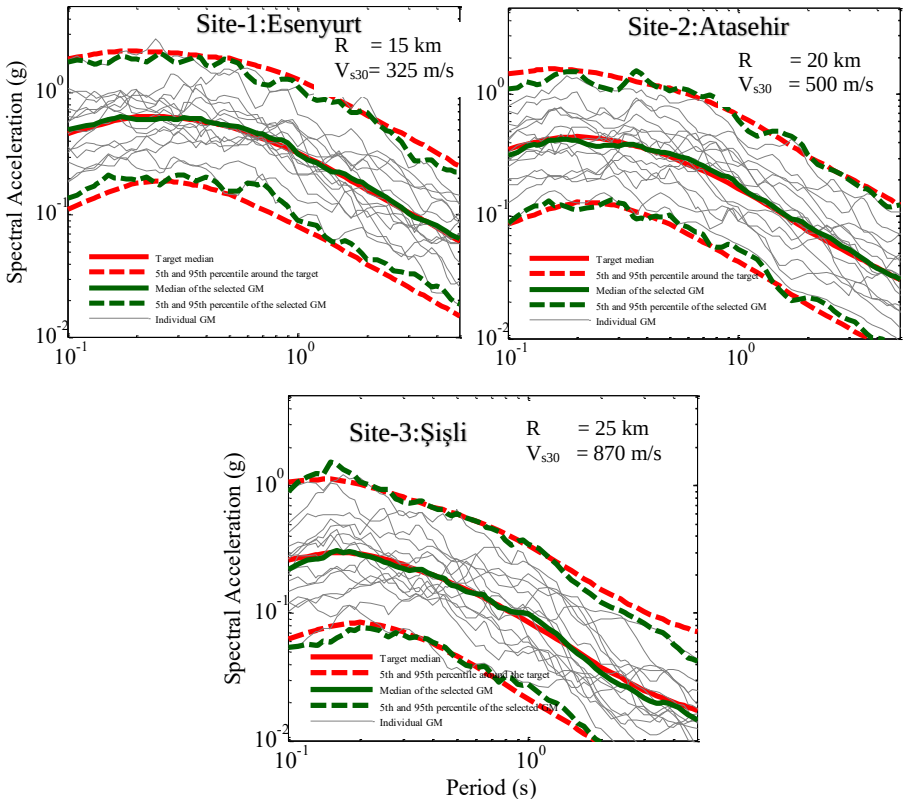

Figure 3. Response spectra of the scaled records matching empirically predicted targets at the three building sites

Physics-based simulations via the SPEED engine

Physics based simulations that are herein used are composed of two wave signals superimposed into a single broadband (referred to as BB hereafter) ground motion: deterministic and stochastic. The open-source software package SPEED (SPectral Element in Elastodynamics with Discontinuous Galerkin: http://speed.mox.polimi.it/) simulates the propagation of large-scale

seismic waves considering the coupled effects of a seismic fault rupture, the propagation path through Earth's layers, localized geological irregularities, such as alluvial basins, and soil-structure interaction problems (Mazzieri et al., 2013). However, this signal is devoid of high-frequency content (F>1.25 Hz). In order to generate the BB simulation, which contains the frequency range of engineering interest (between 0.1 to 25 Hz), the deterministic portion is superimposed with a high-frequency waveform trained by artificial neural networks.

Paolucci et al. (2017) produced 17 magnitude M_w=7.2 earthquake ruptures, and the associated broadband simulations across a large collection of sites in Istanbul. We selected 15 out of these 17 scenarios and collected the two-component horizontal acceleration time series at the building sites. The accrued scenarios constitute the same rupture plane in dimension, but their positions vary in a tightly distributed array of locations across the fault plane as illustrated in Figure 4. However, such variation does not result in any significant difference in the causal parameters (such as the source-to-site distance) of the earthquake at the three building sites of interest.

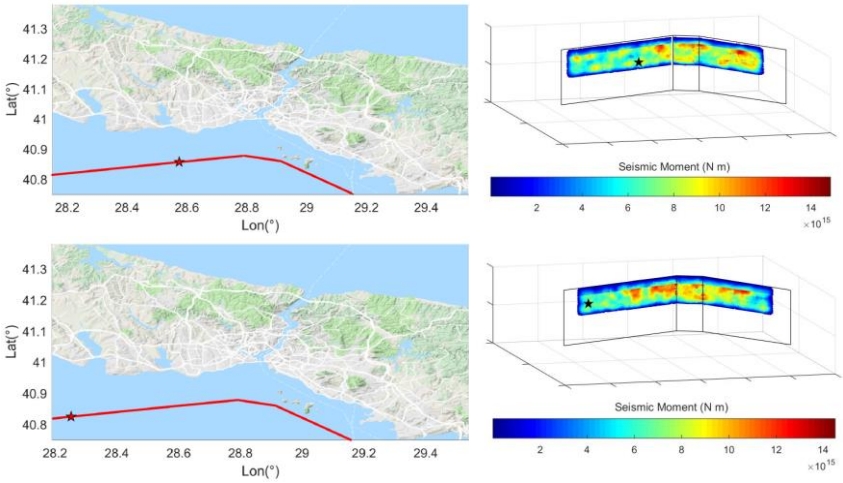

Figure 4. Earthquake scenario simulations. Left panel: projection of the rupture planes (red lines) and the epicentre locations (stars); Right panel: variation in seismic moment.

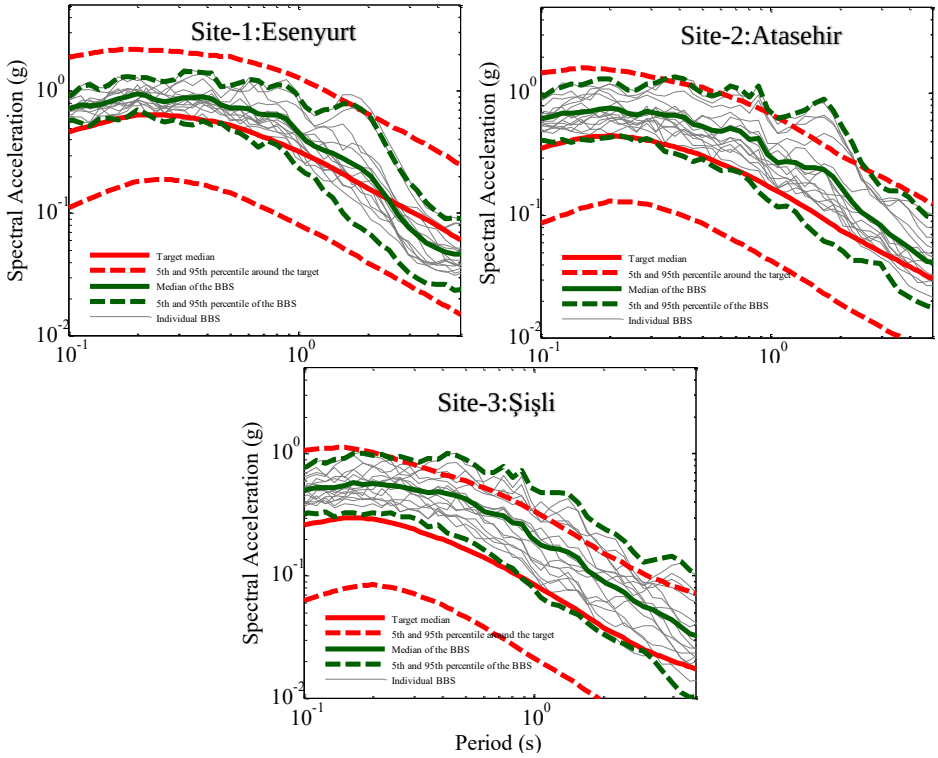

Figure 5. Response spectra of the physics-based ground motion simulations in relation to the empirical predictions at the three building sites

The Sa_{RotD50} response spectra of the BB simulations, which will be used as input time series in dynamic analyses, are presented in Figure 5 . We can observe here that the uncertainty in the spectral accelerations across almost all vibration periods are much smaller compared to the empirical predictions. Dispersion in the shaking appears to be the smallest in Esenyurt, which is the closest site to the rupture. Further, the medians of the PBS spectra are significantly larger than what the GMPM yields. These observations are consistent with those presented in Paolucci et al. (2017).

Archetype tall building and the analysis setting

Model description

The case study structure is a 23-storey, reinforced concrete shear wall building that was designed in accordance to post-1980 seismic design provisions for seismically-active regions. A 3D analytical model of the structure is created in the finite element analysis (FEA) software OpenSees (Mazzoni et al., 2006). The seismic mass and the loads exerted on the structural models are computed as the combination of the dead (invariant) and the expected temporal portion of the live (variant) loads; seismic mass is distributed across floors. Fibre sections are employed by incorporating nonlinear uniaxial constitutive material relations at the section level to simulate the element responses. Expected material (concrete and steel) strength properties are adopted (per PEER, 2017) for accurate representations of both section- and element-level behaviour. Shear response of the elements are mimicked by means of aggregated bilinear springs adopting the shear capacity definitions in Wallace (2007). In the absence of significant deficiencies in the slab systems across archetype buildings, slabs are assumed to exhibit sufficient axial load transfer capabilities, thus their influence is represented by rigid diaphragms across the floors. In order to achieve the best control over the damping forces, a combination of modal damping (2.5% critical across all modes) and Rayleigh damping (0.25% critical at T_1 and T_2) is employed in line with the recommendations in Dierlein et al. (2010). Finally, 3D computer model, its plan view and dynamic properties that are obtained from modal analysis are shown in Figure 6.

Analysis setting

Nonlinear dynamic analyses are performed using the selected records and the physics-based simulations, separately. It should be noted here that the acceleration-time series of the simulated motions exist in east-west and north-south directions, however the two horizontal components of the recorded accelerograms do not always exhibit this feature. Furthermore, the arbitrary assignment of the orientation (across possible azimuths) of the archetype building was also deemed inappropriate for a fair comparison between the two approaches. To this end, in order to reduce potential biases in the seismic demand analyses, acceleration-time series are applied in two separate, perpendicular orientations. In other words, both the records and the simulations are applied first in one arbitrary orientation, and then in the other.

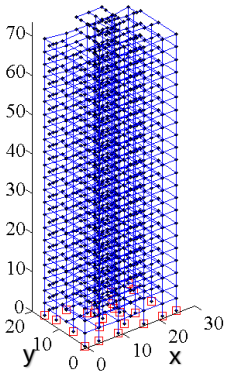

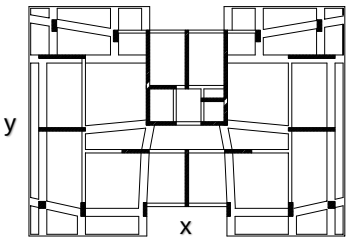

Mode	Period (s)	Mass Participation
1	2.9	0.63 (Torsion)
2	2.5	0.59 (Translational-X
3	2.4	0.65 (Translational-Y)

Figure 6. Mathematical model and dynamic properties of the archetype structure

Analysis results

Using the unique suites of recorded accelerograms and PBS delineating the expected shakings at the building sites, structural response maxima in terms of (1) residual and transient inter-storey drifts, and (2) peak floor accelerations are quantified in the end of the dynamic analyses. Distributions of these demands are presented in Figure 7. It can be clearly seen that the PBS

result in a much lower uncertainty in the responses. Storey drifts appear to be affected to a lesser degree, but the scatter in the floor accelerations are approximately 100 percent smaller given the lognormal assumption. This can easily be traced back to the large difference in the ground motion, especially in shorter vibration periods. Moreover, drifts predicted by the PBS are systematically larger than those predicted via recorded ground motions to a degree that is positively correlated with the residuals in spectral accelerations at the first mode vibration periods of the structure (2.0-3-0s). The residuals in peak floor accelerations, on the other hand, correspond more to the difference at the higher-frequencies (<0.8s).

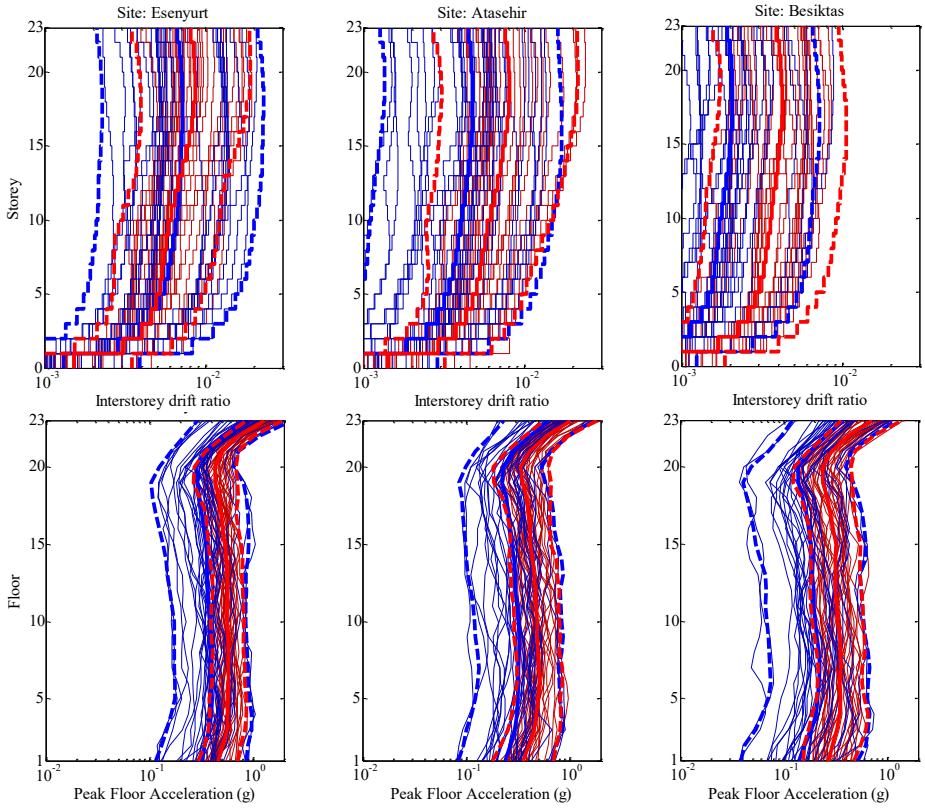

Figure 7. Distributions of structural responses: red lines represent the physics-based simulations, and blue lines represent the recorded motions

Performance evaluations: serviceability and collapse prevention criteria

The Los Angeles Tall Building Structural Design Council (LATBSDC: Brandow et al. 2014) suggests that a maximum transient inter-storey drift ratio of 0.5% can be used as a threshold for delineating serviceability condition of tall buildings in a global sense. It is advocated that it is a good proxy representing the departure from an 'immediate occupancy'*, or '*operational', damage state, which would suggest uninterrupted use of the building after the earthquake, to a 'damaged' condition that would require a minimum level of intervention before the building can be operational again. Further, a storey drift ratio of 4.5% is put forward by the LATBSDC to mark a response threshold after which the structure would become irreparable.

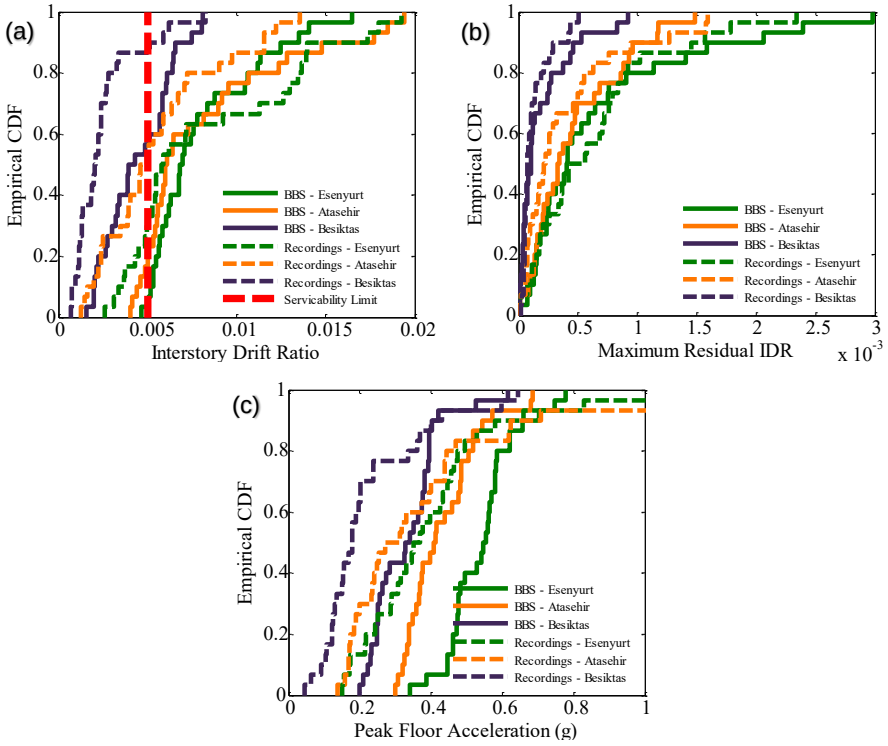

Figure 8. Empirical cumulative distribution functions of (a) maximum transient inter-storey drift ratios, (b) maximum residual inter-storey drift ratios and (c) 15th floor acceleration maxima

Figure 8 presents empirical distributions of (a, b) the maximum transient and residual inter-storey drift ratios and (c) 15th storey peak floor accelerations computed at the three sites via the PBS and the conventional approach using recorded motions. Based on storey drifts, PBS suggest that the scenario shaking at the sites has a 23-to-33% higher chance of inflict repairable damage instead of no damage essentially rendering the building operational (see Table 1). On the other hand, same results also indicated that the structure would not suffer extensive damage that would result in irreparable damage or collapse of the structure.

Structural drifts correlate well with the expected structural damage, but alone, they are not good indicators of economic losses that structures might suffer under low-intensity shakings (Bradley et al., 2008). For example, excessive floor accelerations can result in damage to a considerable collection of the non-structural contents of a structure. Furthermore, the economic value associated to these contents can be expected to significantly greater in tall residential and office buildings compared to low- to mid-rise regular residential houses because of the difference in the luxury levels (Papadopoulos et al., 2018). Unfortunately, the literature lacks solid research on the side of a sufficient indicator, which considers both drifts and floor accelerations, for estimating economic loss. However, based upon the garnered loss data after the 1999 earthquakes in Turkey, Bal et al. (2008) suggested that the economic losses can be predicted to be within the range of 16-to-33% of the total replacement cost of a structure that suffered slight-to-moderate damage, which can be placed under the umbrella of the *repairable* damage state. These values correspond to expected repair costs associated to retrofitting.

For simplicity, let's assume that the expected economic losses corresponding to a slight-to-moderate damage state in a tall building would be 25%. Invoking the law of total expectation, we can compute the expected losses given the scenario event, $L_{M=7.2}$, *as follows:*

$$E(L_{rup}) = \sum_{i}^{nDS} E(L_{rup}|DS_i).P(DS_i) \quad (1)$$

In Equation 1, $E(L_{rup})$ represents the expected loss given the considered scenario magnitude M=7.2 event; DS_i represents the i^{th} damage state amongst those listed in Table 1. We compute that the expected losses can be as high as 23% of the total replacement costs of the tall buildings in the most hazardous site, Esenyurt. Conversely in Şişli, where the hazard is relatively lower but the land value is amongst the highest across the city, the expected loss ratio is 10% (Table 1).

Finally, note that these values are obtained via the PBS; the conventional method predicts the losses to be 25-to-70% less under the same causal earthquake.

	Global Damage State Probabilities (in %)			Losses
	Operational	Repairable	Irreparable or collapse	Ratio of loss to total replacement cost
Esenyurt	7 | 30	93 | 70	0 | 0	0.232 | 0.175
Atasehir	20 | 53	80 | 47	0 | 0	0.200 | 0.117
Şişli	58 | 88	42 | 12	0 | 0	0.105 | 0.030

Table 1. Global damage state probabilities, based on maximum inter-storey drifts per LATBSDC, and loss ratios. Red and blue coloured texts correspond to the results obtained via PBS and the conventional approach, respectively.

Conclusions

In this paper, we evaluated the seismic performance of a 23-storey archetypal tall building, which was designed as per post-1980 modern capacity design principles, at three different sites in Istanbul under a magnitude M=7.2 earthquake rupture scenario. These sites constituted locations where tall buildings are densely populated, and the seismic hazard characteristics varied. Considering the seismic gap in the Sea of Marmara, the considered earthquake scenario was deemed a potential rupture that would manifest itself as the 'next big one'.

The physics-based broadband ground motion simulations, which are generated by Paolucci et al. (2017) using the spectral element code SPEED, at the building sites due to the scenario earthquake are used to perform nonlinear dynamic analyses and compute the seismic demands and assess structural performance. The same task is undertaken also via conventional methods that use recorded ground motions as input time series for dynamic analyses. We observed that:

1. There is a significant difference in the empirically predicted versus numerically simulated ground shaking at the three sites of interest. The simulated suites of ground motions are more aggressive in terms of spectral accelerations compared to those selected and scaled matching the target spectra predicted by the ground-motion predictive model. The physics-based simulations (PBS) exhibit half the dispersion in the shaking intensity that the selected records do.
2. The differences in the shaking intensities carry over to the responses. Further, PBS, in comparison with the conventional approach, result in much higher floor accelerations than it does so in storey drifts. That is to say that the difference across approaches manifest itself more clearly in floor accelerations rather than storey drifts.
3. Economic losses that the archetype tall building might suffer due to the scenario event were predicted to average between: 10-to-23% via PBS, and 3-to-18% via the conventional approach depending on the building site.
4. Overall, both methodologies predict that the probability of collapse or the occurrence of damage beyond repair is zero.

Acknowledgements

The first author gratefully acknowledges the financial support provided by the University School of Advanced Studies of Pavia (IUSS Pavia).

References

Ambraseys, N.N., Finkel, C.F., 1991. Long Term Seismicity of Istanbul and of the Marmara Sea Region. Terra Nov. 3.

Baker, J.W., Luco, N., Abrahamson, N.A., Graves, R.W., Maechling, P.J., Olsen, K.B., 2014. Engineering Uses of Physics-Based Ground Motion Simulations, in: Tenth U.S. National Conference on Earthquake Engineering. Alaska.

Bal, İ.E., Crowley, H., Pinho, R., Gülay, F.G., 2008. Detailed assessment of structural characteristics of Turkish RC building stock for loss assessment models. Soil Dyn. Earthq. Eng. 28, 914–932. https://doi.org/10.1016/J.SOILDYN.2007.10.005

Bohnhoff, M., Martínez-Garzón, P., Bulut, F., Stierle, E., Ben-Zion, Y., 2016. Maximum

earthquake magnitudes along different sections of the North Anatolian fault zone. Tectonophysics 674, 147–165. https://doi.org/10.1016/j.tecto.2016.02.028

Boore, D.M., Stewart, J.P., Seyhan, E., Atkinson, G.M., 2014. NGA-West2 Equations for Predicting PGA, PGV, and 5% Damped PSA for Shallow Crustal Earthquakes. Earthq. Spectra 30, 1057–1085. https://doi.org/10.1193/070113EQS184M

Boore, D.M., Watson-Lamprey, J., Abrahamson, N.A., 2006. Orientation-Independent Measures of Ground Motion. Bull. Seismol. Soc. Am. 96, 1502–1511. https://doi.org/10.1785/0120050209

Bradley, B., Baker, J.W., 2014. Ground motion directionality in the 2010-2011 Canterbury earthquakes. Earthq. Eng. Struct. Dyn. https://doi.org/10.1002/eqe.2474

Bradley, B.A., Dhakal, R.P., Cubrinovski, M., Macrae, G.A., Lee, D.S., 2008. Seismic loss estimation for efficient decision making. NZCEE.

Bradley, B.A., Pettinga, D., Baker, J.W., Fraser, J., 2017. Guidance on the Utilization of Earthquake-Induced Ground Motion Simulations in Engineering Practice. Earthq. Spectra 33. https://doi.org/10.1193/120216EQS219EP

Brandow, G., Carpenter, L., Cochran, B.L., Hart, G.C., Huang, S.C., Lew, M., Martin, J. a, Naeim, F., Pinkham, C.W., Sabol, T., Schindler, B., Strand, D.R., Youssef, N., 2014. An Alternative Procedure for Seismic Analysis and Design of Tall Buildings Located in the Los Angeles Region (LATBSDC).

Dierlein, G.G., Reinhorn, A.M., Willford, M.R., 2010. Nonlinear Structural Analysis For Seismic Design A Guide for Practicing Engineers. California.

Dönmez, C., Pujol, S., 2005. Spatial distribution of damage caused by the 1999 earthquakes in Turkey. Earthq. Spectra 21, 53–69. https://doi.org/10.1193/1.1850527

Erdik, M., Demircioglu, M., Sesetyan, M., Durukal, E., Siyahi, B., 2004. Earhtquake hazard in Marmara Region, Turkey, in: 13th World Conference on Earthquake Engineering. Vancouver, B.C.

Graves, R., Jordan, T.H., Callaghan, S., Deelman, E., Field, E., Juve, G., Kesselman, C., Maechling, P., Mehta, G., Milner, K., Okaya, D., Small, P., Vahi, K., 2011. CyberShake: A Physics-Based Seismic Hazard Model for Southern California. Pure Appl. Geophys. 168, 367–381. https://doi.org/10.1007/s00024-010-0161-6

Mazzieri, I., Stupazzini, M., Guidotti, R., Smerzini, C., 2013. SPEED: SPectral Elements in Elastodynamics with Discontinuous Galerkin: a non-conforming approach for 3D multi-scale problems. Int. J. Numer. Methods Eng. 95, 991–1010. https://doi.org/10.1002/nme.4532

Mazzoni, S., Mckenna, F., Scott, M.H., Fenves, G.L., Iii, A., 2006. Open System for Earthquake Engineering Simulation (OpenSees) OpenSees Command Language Manual.

Paolucci, R., Mazzieri, I., Ozcebe, A.G., Smerzini, C., Stupazzini, M., Infantino, M., 2017. 3D Physics-based earthquake scenarios in Istanbul for seismic risk assessment, in: 16th World Conference on Earthquake Engineering. Chile. https://doi.org/N° 1478

Paolucci, R., Mazzieri, I., Smerzini, C., 2015. Anatomy of strong ground motion: Near-source records and three-dimensional physics-based numerical simulations of the Mw 6.0 2012 may 29 po plain earthquake, Italy. Geophys. J. Int. 203, 2001–2020. https://doi.org/10.1093/gji/ggv405

Papadopoulos, A.N., Vamvatsikos, D., Kazantzi, A.K., 2018. Development and application of FEMA P-58 compatible story loss functions. Earthq. Spectra. https://doi.org/10.1193/020518EQS033M

Parsons, T., Toda, S., Stein, R.S., Barka, A., Dieterich, J.H., 2000. Heightened Odds of Large Earthquakes Near Istanbul: An Interaction-Based Probability Calculation. Science (80-.). 288, 661–665.

PEER, 2017. Tall Buildings Initiative: Guidelines for Performance - Based Seismic Design of Tall Buildings, PEER Report 2017/06. California.

Shahi, S.K., Baker, J.W., 2011. An empirically calibrated framework for including the effects of near-fault directivity in probabilistic seismic hazard analysis. Bull. Seismol. Soc. Am. 101, 742–755. https://doi.org/10.1785/0120100090

Somerville, P.G., Smith, N.F., Graves, R.W., Abrahamson, N.A., 1997. Modification of Empirical Strong Ground Motion Attenuation Relations to Include the Amplitude and Duration Effects

of Rupture Directivity. Seismol. Res. Lett. 68, 199–222. https://doi.org/10.1785/gssrl.68.1.199

Tarbali, K., Bradley, B.A., Huang, J., Polak, V., Lagrava, D., Motha, J., Sung, S., 2018. Cybershake NZ v17 . 9 : New Zealand simulation-based probabilistic seismic hazard analysis.

Wallace, J.W., 2007. Modelling Issues for Tall Reinforced Concrete Core Wall Buildings. Struct. Des. Tall Spec. Build. 16, 615–632. https://doi.org/10.1002/tal.440

Wood, H.O., Neumann, F., 1931. Modified Mercalli Intensity Scale of 1931. Bull. Seismol. Soc. Am. 21, 277–283.